PCCP

Accepted Manuscript

ROYAL SOCIETY OF CHEMISTRY

www.rsc.org/pccp

Physical Chemistry Chemical Physics
CREATED USING THE RSC LaTeX PCCP ARTICLE TEMPLATE – SEE www.rsc.org/electronicfiles FOR DETAILS
ARTICLE TYPE www. rsc.org/xxxxxx | XXXXXXXX

The nature of bonding and electronic properties of graphene and benzene with iridium adatoms

Petr Lazar,[a] Jaroslav Granatier,[bc], Jiri Klimes[d], Pavel Hobza[b] and Michal Otyepka*[a]

Received Xth XXXXXXXXXX 20XX, Accepted Xth XXXXXXXXX 20XX
First published on the web Xth XXXXXXXXXX 200X
DOI: 10.1039/b000000x

Recent theoretical simulations predicted that graphene decorated with Ir adatoms could realize a two-dimensional topological insulator with a substantial band gap. Our understanding how the electronic properties of graphene change under a presence of metal adatoms is however still limited, as the binding is quite complex involving static and dynamic correlation effects together with relativistic contributions, which makes a theoretical description of such systems quite challenging. We applied quantum chemical complete active space second order perturbation theory (CASPT2) method and density functional theory beyond the standard local density functional approach including relativistic spin-orbit coupling (SOC) effects to Ir-benzene and Ir-graphene complexes. The CASPT2-SOC method revealed a strong binding of the Ir to benzene (33.1 kcal/mol) at 1.81 Å distance, which was of a single reference character, and a weaker binding (6.3 kcal/mol) at 3.00 Å of a multireference character. In the Ir-graphene complex, the quartet ground-state of the Ir atom changed to the doublet state upon adsorption, and the binding energy predicted by optB86b-vdW-SOC functional remained high (33.8 kcal/mol). In all cases the dynamic correlation effects significantly contributed to the binding. The density of states calculated with the hybrid functional HSE06 showed that the gap of 0.3 eV was induced in graphene by the adsorbed Ir atom even in scalar relativistic calculation, in contrast to metallic behaviour predicted by local density approximation. The results suggest that the strong correlation effects contribute to the opening of the band gap in graphene covered with the Ir adatoms. The value of the magnetic anisotropy energy of 0.1 kcal/mol predicted by HSE06 is lower than those calculated using local functionals.

1 Introduction

Graphene is a material that has been demonstrated to have promising applications in diverse disciplines, ranging from electronics to medicine.[1–3] Graphene is among the candidate materials for post-silicon electronics, however the creation of graphene-based electronic devices requires opening of the zero bandgap in graphene.[4] Graphene also serves as a prototype of two-dimensional topological insulator,[5] as the existence of the quantum spin Hall effect was first suggested for pure graphene after the effects of spin orbit interactions have been considered.[6] Topological insulators are distinct from simple band insulators; their insulating state has topologically non-trivial band structure, which is manifested by a nonzero spin Hall response arising from metallic edge states protected against perturbations by time-reversal symmetry.[7] Unfortunately, spin-orbit coupling in carbon is very weak, making the gap in pure graphene extremely small from the application point of view.

However, the application potential of graphene can be extensively broadened by various modes of functionalization, which usually comprise adsorption of atoms, molecules or nanoparticles.[8] In this respect, recent theoretical study by Hu et al.[9] indicated that graphene covered with heavy adatoms (Os and Ir) can behave like giant topological insulator protected by a large gap. Moreover, there seems to be a way how to prepare iridium covered graphene, as earlier experiments showed that lattices of Ir nanoclusters can be grown on graphene by chemical vapor deposition.[10] The nature of iridium-graphene interaction is not however fully clear; density functional theory calculations based on the generalized gradient approximation (GGA) predicted the shape of grown iridium clusters at variance with experimental observation.[10] No wonder, as the systems of adatoms or atomic clusters on graphene belong among the cases where the limitations of local density approximations in DFT can be severe.[11–13] The interaction of graphene with atoms such as Ir may be mediated by the effects going beyond the realm of the traditional DFT method, in particular multi-configurational nature of the wavefunction arising from close-lying states of the iridium atom.

[a] *Regional Centre of Advanced Technologies and Materials, Department of Physical Chemistry, Faculty of Science, Palacky University Olomouc, tr. 17. listopadu 12, 771 46 Olomouc, Czech Republic.*
[b] *Institute of Organic Chemistry and Biochemistry, Academy of Sciences of the Czech Republic, Flemingovo nm. 2, 166 10 Prague 6, Czech Republic.*
[c] *Institute of Physical Chemistry and Chemical Physics FCHPT, Slovak University of Technology, Radlinskeho 9, Bratislava SK-812 37, Slovakia.*
[d] *University of Vienna, Faculty of Physics and Center for Computational Materials Science, Sensengasse 8/12, A-1090 Vienna, Austria*

Thus detailed understanding of the iridium-graphene interactions should help to resolve these issues and better asses potential application of iridium covered graphene.

We present a detailed study of Ir-arene complexes aimed to uncover the nature of bonding between iridium atoms and graphene. We started with the Ir-benzene half-sandwich complex as a simple model system, which allows to utilize elaborate techniques of quantum chemistry. Specifically, we applied state-of-the-art multi-reference method, the Complete Active Space Second Order Perturbation Theory (CASPT2).[14,15] Apart from using multi-reference description of the wavefunction, the CASPT2 method involves static as well as dynamic correlations, and therefore allows to treat systems problematic in traditional DFT, such as those involving strong correlation, bond breaking reactions, and transition metals.[16]

The results in the first section reveal that the potential energy surfaces can be divided into two areas with different character of bonding. As the Ir atom approaches benzene, shallow local minimum of the energy occurs at first. This area is characterized by mixing of close lying states and the multi-reference approach is necessary for the construction of the wavefunction. The four most stable states correspond to quartet states of the Ir atom interacting with benzene. The next area lies around the position of the global energy minimum at the bonding distance of 1.8 Å. The most stable state in this area arises from the interaction between the benzene molecule and quartet ^{4}F state with $5d^8 6s^1$ electron configuration of the Ir atom. This configuration dominates the wavefunction in the area and therefore the electronic structure can be described by single-reference methods with a good accuracy. The ground-state $5d^7 6s^2$ configuration does not contribute to the bonding.

In the second section, we utilize the results obtained for benzene and calculate the potential energy curves for the adsorption of the iridium atom on graphene. The results show that the absorption of Ir atoms is non-activated process, with the adsorption energy and equilibrium distance similar to those on benzene. We calculated the density of states in incremental series of approximations, starting with local density approximation, over generalized gradient approximation up to the screened hybrid functional. The density of states, the net magnetic moment, and the splitting of *d* states at the Fermi level, strongly depend on the functional used. The value of the net magnetic moment in the complex calculated by HSE06 corresponds to the doublet state, in contrast to the LDA functional, which predicts that the magnetic moment is completely quenched. Hybrid functional HSE06 also lowers very large magnetocrystalline anisotropy predicted by local functionals.

The density of states calculated by HSE06 has a gap of 0.3 eV at the Fermi level without spin-orbit coupling, whereas both LDA and GGA yield gapless density of states in scalar relativistic limit. When the spin-orbit interaction is present, the gap size depends on the orientation of the spin quantization axis. Aligning the axis along one of the directions within graphene sheet, the degeneracy of d_{xz} and d_{yz} states is lifted and the gap amounts to 0.31 eV, the value essentially identical to scalar relativistic case. Alignment perpendicular to graphene increases the gap to the value of 0.45 eV.

2 Results and discussion

2.1 Ir-benzene

The two lowest-lying states of the Ir atom are ^{4}F states. While the ground ^{4}F state corresponds to the $5d^7\ 6s^2$ electron configuration, the electron configuration of the first excited ^{4}F state is $5d^8\ 6s^1$.[17] We applied CASPT2 and its multi-state variant MS-CASPT2 for the calculations of the interaction between benzene and the Ir atom in doublet and quartet states. Resulting potential energy curves are displayed in Figure 1. We can divide them into two areas according to the character of bonding. The first area lies around the position of the global energy minimum, which is at the bonding distance of 1.8 Å. The most stable state in this area arises from the interaction between the benzene molecule and quartet ^{4}F state with $5d^8 6s^1$ electron configuration of the Ir atom. The analysis of configurations and their coefficients showed that this is dominant configuration in the first area and therefore the electronic structure in this area can be described by single-reference methods with a good accuracy.

The CASPT2 and MS-CASPT2 binding energies and distances of this quartet state are essentially identical, 43.1 (1.79 Å) and 43.3 kcal/mol (1.80 Å), respectively. The interaction energy of 43 kcal/mol is considerably higher than the interaction energies in coinage metals-benzene[11] and even in Pt-benzene[18]. The binding energy of the second most stable state, which corresponds to the doublet state, is by 8 kcal/mol lower. The analysis of the hybridization of states in the first area reveals similar nature of bonding as observed in the Pd-benzene and Pt-benzene complexes.[11,18] The Ir atom is bonded to benzene by a dative bond characterized by strong direct charge transfers from iridium *d*-orbitals to benzene and the backward charge transfer from benzene to 6p orbitals of the Ir atom. As a result, the Ir atom is negatively charged, whereas the benzene molecule acquires positive charge at the CASPT2 level. The resulting charge at the Ir atom is 0.52 *e*. It is worth noting that the CASSCF method, which omits dynamic electron correlation, provides positive interaction energies (no bonding between the Ir atom and benzene). Similar charge transfer appears at the CASSCF level as well, but it is not strong enough to counterbalance repulsion. Thus, dynamic electron correlation is necessary for the attraction between the Ir atom and benzene molecule to appear.

The second area is found around bonding distances of 3 Å,

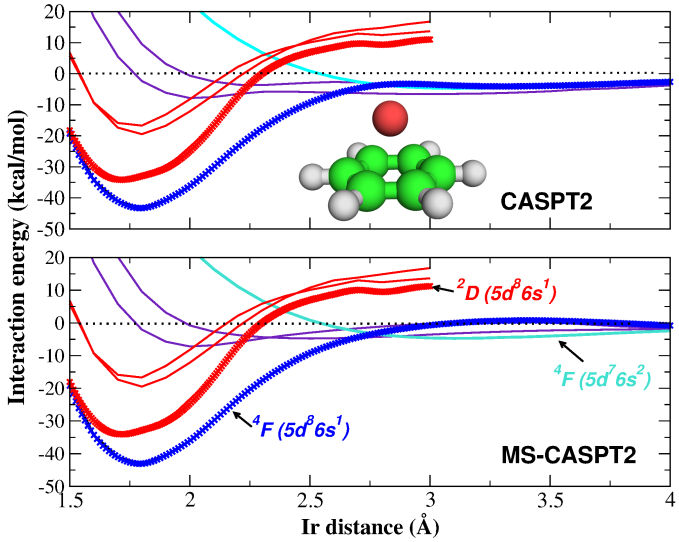

Fig. 1 The potential energy surfaces of low-energy quartets (light blue: ground state a^4F, blue: a^4F) and doublet (thick red) iridium states in the Ir-benzene complex. Thin red and violet curves are higher lying quartet and doublet states, respectively. Upper panel: CASPT2 method and the sketch of the Ir-benzene complex, lower panel: multi state CASPT2.

where the CASPT2 curves feature the shallow local minimum of the energy. This area is characterized by mixing of close lying states. The multi-reference approach is thereby necessary for the construction of the wavefunction and correct description of the interaction. The four most stable states correspond to quartet ^{4}F states of the Ir atom interacting with benzene. The electron configuration of these states is analogous to the configuration in the global minimum - $5d^8 6s^1$. The CASPT2 and MS-CASPT2 binding energies and distances of the most stable of quartet states are 4.7 kcal/mol at 3.13 Å and 6.6 kcal/mol at 3.00 Å, respectively. Also in the second area, the Ir atom is charged negatively with charge about 0.1 *e*. However, the carbon atoms of benzene are also charged negatively (about 0.04 *e*). The bonding in this area can be characterized as van der Waals interaction.

Notice that the shallow local minimum of the potential energy is usually associated with physisorption state and is typically found when molecules adsorb onto solid surfaces. The nature of the shallow minimum at 3.00 Å in the Ir-benzene complex is more complex; the van der Waals interaction is accompanied by intermixing of close-lying quartet states, as illustrates Figure 1. It should be noted that the second minimum of potential energy curve corresponding to a metastable precursor state was observed experimentally for benzene adsorbing on Ir (and Pt) surfaces.[19]

The CASPT2 results enable to gauge the ability of DFT functional to desribe the interaction of the Ir atom with benzene. We started with a simple DFT calculation of the potential energy surface of the Ir-benzene complex with the most common functional being used nowadays, generalized gradient parametrized by Perdew-Burke-Ernzerhof (PBE).[20] Figure 2 depicts calculated potential energy curve. The bonding distance of 1.8 Å obtained from PBE corresponds well to the bonding distance predicted by the CASPT2 method (Figure 1), owing to the single-reference character of the wavefunction in the minimum. The calculation also correctly reproduces that quadruplet groundstate multiplicity of the iridium atom does not change at the equilibrium bonding distance. On the other hand, the interaction energy of 34.9 kcal/mol is lower than the CASPT2 value (43.1 kcal/mol). Furthermore, multi-reference character of the system manifested itself in the area of the second minimum, because the self-consistent cycle used to solve the total energies in DFT did not converge in that range of Ir distances. (Supporting Information, Figure 1a). The diagonalization algorithm in VASP, Davidson block iteration scheme, produced discontinuous potential energy curve and even diverged at some distances. The behaviour is caused by the presence of close-lying states along potential energy curve in this region (Figure 1). It is worth noting that we obtained convergent and physically reasonable potential energy curves by setting the smearing to 0.01 eV and by switching to all bands simultaneous diagonalization (see Supporting Information for details). The resulting potential energy curves show no signs of the second minimum. This is expected behavior, because the PBE functional does not cover any non-local dispersive interactions.

Interestingly, the second minimum along potential energy pathway is absent even when vdW-DF functionals were used. The comparison of classical DFT functionals (LDA and GGA), and modern van der Waals corrected functionals optB86b-vdW and optB88-vdW with the CASPT2 result is displayed in Figure 2. None of the functionals yields the second minumum, which may reflect its multi-reference character. Optimized vdW-DF functionals provide better description of energetics of the Ir decay into vacuum, which is always mediated by van der Waals interactions. This becomes important when the interaction forces, instead of energies, are in question.[21] On the other hand, all functionals predict correct equilibrium bonding distance of 1.8 Å, despite pronounced differences in the bonding energy. This is a positive surprise especially in the case of LDA, since in noble metal-benzene complexes, using LDA lead to unphysically strong hybridization of metal-benzene states and, consequently, the bonding distances were too short.[11] The energy of bonding is strongly overestimated by LDA, a deficiency of this approximation which is well known from its condensed matter applications. Here, classical PBE functional (inset of Figure 2) offers great

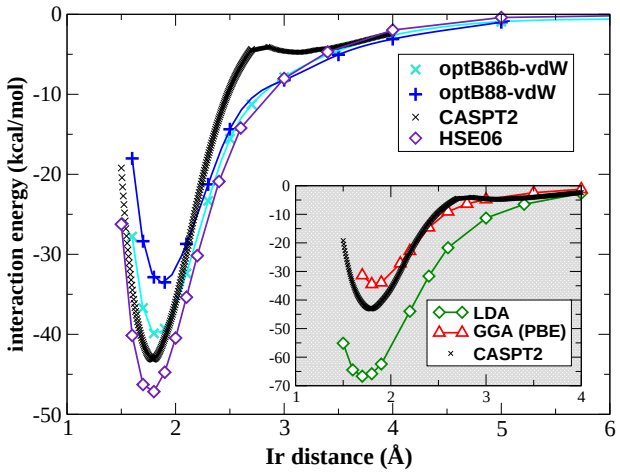

Fig. 2 The total energies of the Ir-benzene complex as a function of the distance calculated by optimized van der Waals functionals (optB86b-vdW and optB88-vdW) and hybrid functional HSE06 compared to the CASPT2 result. Inset: classical LDA and GGA functionals compared to CASPT2.

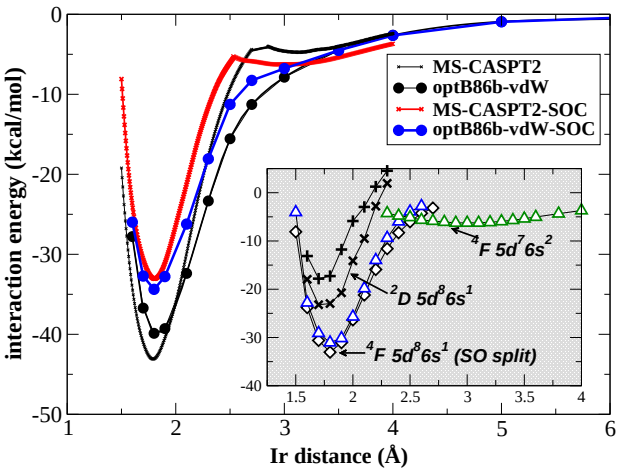

Fig. 3 The potential energy surface in the Ir-benzene complex as a function of Ir distance - the influence of spin-orbit coupling on the optB86b-vdW van der Waals functional (blue) and multi-state CASPT2 (red). The scalar relativistic results are depicted for comparison (in black). Inset: quartet and doublet states in the Ir-benzene complex according to MS-CASPT2-SOC.

improvement over LDA, as its binding energy of 34.9 kcal/mol gets closer to CASPT2 value. Further improvement comes from optB86b-vdW functional, which yields the binding energy of 40.1 kcal/mol, just slightly lower than CASPT2 result, and can be recommended for treatment of the adsorption of Ir atoms on arenes.

All of DFT functionals also predict that no spin-crossing occurs and the quartet state is the ground-state of the Ir atom in the complex, in agrement with the CASPT2 calculations (although the quartet states are intermixed, Figure 1). That seems to be rather exceptional, because spin is more often quenched in metal/arene complexes. Specifically, Sargolzaei and Gudarzi showed that magnetic moments of 3*d* transition-metal atoms added to the surface of graphene and benzene are partially quenched compared to their free atomic state, apart from Co adatom on graphene and benzene, and Cr adatom on benzene.[22] Similarly, triplet state of platinum is quenched in benzene[18] or graphene[23] complexes. Spin quenching also affects small metal clusters interacting with graphene.[12]

The factor which remains to be considered is the spin-orbit coupling (SOC), a higher order relativistic effect. Figure 3 shows that the character of the Ir-benzene interaction is not affected by the spin-orbit coupling, i.e. the spin-orbit interaction does not change the ordering of states. The quartet state remains the minimum along the potential energy pathway. Spin-orbit interaction only leads to the lowering of the interaction energy, in particular the energy of the first minimum, which is decreased to 33.1 kcal/mol at the 1.81 Å at the MS-CASPT2-SOC level. This finding is in agreement with the DFT results, because no qualitative changes of the interaction energies occur in DFT calculation. The spin-orbit coupling increases the DFT interaction energies by a similar amount as in the case of MS-CASPT2-SOC calculation. The optB86b-vdW-SOC functional gives the interaction energies in very good agreement with the MS-CASPT2 energies in the global minimum (Figure 3). On the other hand, the effect of spin-orbit coupling to the second minimum is small. Its binding energy is 6.3 kcal/mol at the 3.00 Å at the MS-CASPT2-SOC level. Thus, the spin-orbit coupling decreases the stability of the Ir-benzene complex, especially in the first minimum.

2.2 Ir-graphene

The adsorption of Ir on graphene is very similar to the adsorption on benzene. The potential energy curves are displayed in Figure 4 (the iridium atom was again placed into the hollow position). The equilibrium bonding distance of 1.8 Å agrees almost exactly with the value found on benzene. The binding energies provided by the optB86b-vdW functional (33.8 kcal/mol in scalar relativistic calculation and 24.9 kcal/mol with spin-orbit coupling included) are lower than those on

benzene, but still high enough to indicate that the d orbitals of iridium partly overlap with p states of graphene. The spin-orbit coupling decreases the stability of the Ir-graphene complex. Obviously, the main characteristics of adsorption are very similar to the Ir-benzene complex.

The hybridization of graphene p-states with d-states of iridium results in strong modification of graphene density of states. Typical linear dispersion of states around the Dirac cone is spoiled by the presence of localized iridium states. Figure 4 shows that scalar relativistic LDA yields gapless density of states, in agreement with the study by Hu et at.[9] The important feature is the peak lying directly at the Fermi level, arising from overlapping p_z and $d_{xz/yz}$ states. Hu et al.[9] argued that spin-orbit interaction splits this peak and a gap opens slightly below the Fermi level. However, the size of the gap and its position with respect to the Fermi level can be strongly influenced by the functional used. It is well known that LDA (and GGA, in lesser amount, as well) calculates incorrectly the gaps between valence and conducting bands of typical semiconductors, or insulators. These methods underestimate the energy of localized d states due to the self-interaction error and, consequently, tend to predict d states to be too delocalized.[24]

We resolve this issue by calculating the density of states in several approximations, starting with LDA, over optB86b-vdW (which uses GGA for the exchange part) up to the screened hybrid functional HSE06, and consider the effect of the spin-orbit coupling in each approximation.

The densities of states calculated with out-of-plane magnetic axis are displayed in Figure 5. Our LDA calculation reproduces the spin-orbit induced splitting of $d_{xz/yz}$ manifold at the energy 0.5 eV below the Fermi level reported by Hu et al.[9] The optB86b-vdW functional provides similar character of the density of states around the Fermi level; the spin-orbit interaction splits $d_{xz/yz}$ states and creates small gap of 0.12 eV at the energy 0.5 eV below the Fermi level. The HSE06 functional shows strikingly different picture. The density of d-states is depleted around the Fermi level and the $d_{xz/yz}$ peaks become much more localized. The gap below the Fermi level disappears. More importantly, a gap opens just above the Fermi level, because $d_{xz/yz}$ states are pushed to higher energies. The gap size is 0.45 eV.

The question now arises whether large gap given by HSE06 stems from the spin-orbit interaction or from reduced self-interaction error in hybrid functional. To answer it we calculated the density of states by HSE06 also in scalar relativistic approximation, which implicitly assumes zero spin-orbit term. We also aligned spin-quantization axis along the in-plane direction to uncover directional-dependency of the electron structure. The results are summarized in Figure 6. The splitting of d-states above the Fermi level is reproduced even in scalar relativistic calculation (bottom panel). Corresponding gap is 0.3 eV wide. Switching on spin-orbit term with quantization axis along the out-of-plane direction (upper panel), the gap becomes slightly wider (0.45 eV) and the antibonding $d_{xz/yz}$-states get higher in energy. Aligning the axis along the in-plane direction, the degeneracy of d_{xz} and d_{yz} states is broken (middle panel). Consequently, d_{yz} states are pushed to lower energies and their density close to the Fermi level is depleted. The main feature at the Fermi level are then d_{xz} states hybridized with p_z states of graphene. The gap of 0.31 eV is very similar to the gap obtained in scalar relativistic calculation. According to Figure 6, the orientation of the quantization axis considerably influences the electronic structure and should be taken into account in investigations involving heavy elements on graphene.

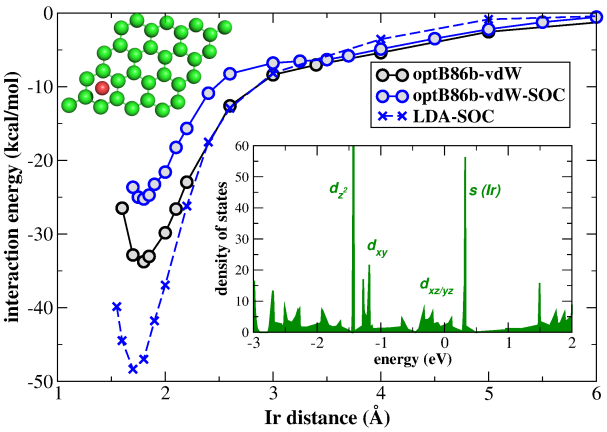

Fig. 4 The interaction energy of the Ir-graphene complex as a function of Ir distance calculated with optimized van der Waals functionals within scalar relativistic approximation (optB86b-vdW) and with spin-orbit coupling included (optB86b-vdW-SOC). Inset: the density of states of the the Ir-graphene complex calculated with the LDA functional within scalar relativistic approximation showing that no gap occurs at the Fermi level (aligned to E=0 eV in figure), and the supercell of the Ir-graphene system (upper left).

These findings indicate that the gap is not opened exclusively due to the spin-orbit interaction. This behaviour is in stark contrast to scalar relativistic calculation using LDA/GGA functionals, in which no splitting of d-states occurs in the vicinity of the Fermi energy. LDA and GGA density functionals dramatically underestimate the band gaps for insulators because they fail to reproduce a derivative discontinuity of the energy with respect to the number of electrons.[24] This behaviour has been already observed in many transition metal oxides, in which local functionals even incorrectly predict a metallic groundstate, although strong Coulomb repulsion between d-electrons makes the oxides wide-band gap in-

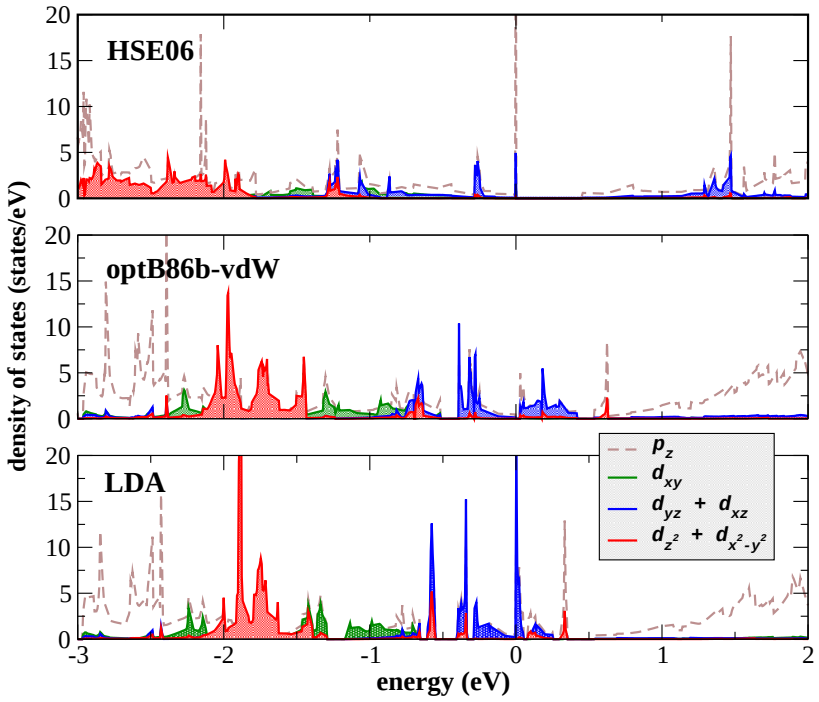

Fig. 5 The density of states of the Ir-graphene complex calculated including spin-orbit coupling and exchange-correlation functional a) LDA, b) optB86b-vdW (which analogical to PBE when density of states is of concern) and c) hybrid HSE06.

sulators. Hybrid functionals include exact Hartree-Fock exchange that corrects this behavior, improves the position of the *d* band, and gives band gaps close to the experiment.[25–27]

Furthermore, the spin-orbit coupling decouples the spin and orbital magnetic moments and causes finite magnetocrystalline anisotropy of the Ir-graphene system. We found that the preferred orientation of the spin quantization axis lies along the direction perpendicular to the graphene plane (out-of-plane), in agreement with previous theoretical study.[28] The parallel orientation (in-plane) has the total energy higher by 0.3, 0.37, and 0.12 kcal/mol as calculated by the LDA, optB86b-vdW, and HSE06 functional, respectively. Obviously, orbital-dependent HSE06 functional reduces large magnetocrystalline anisotropy energy predicted by (semi-) local functionals. It should be noted that we do not consider the dependence of the anisotropy energy on the orientation of the magnetization within the plane of graphene, which is assumed to be very small because of the high in-plane symmetry. The anisotropy energy of 0.12 kcal/mol is too small for spintronic applications, but it can be greatly improved by adsorbing heteronuclear transition metal dimers on graphene.[29,30]

Magnetocrystalline anisotropy of materials has received great attention recently,[31,32] owing to its importance for magnetic storage devices, however the influence of exchange-correlation functional has not been in question often. Blonski and Hafner compared the results of PBE and HSE functionals for Ni, Pd, and Pt dimers; HSE left the spin and orbital moments essentially unchanged but reduced the magnitude of the anisotropy energy in all dimers.[33] Recent study of Os adatoms adsorbed on finite graphene flakes compared PBE with hybrid functional B3LYP and found similar trend - the spin moments were slightly increased by the hybrid, but the anisotropy energy was lowered.[34]

Our findings are in line with these results. According to Table 1, HSE06 yields higher spin as well as orbital moments than its local counterparts, yet the anisotropy energy is lower as observed aforementioned studies. This result can be understood on basis of the energy lowering due to the spin-orbit coupling, which can be expressed in simplified form as[35]

$$\Delta E_{SOC} \propto \sum_{u,o} \frac{\langle u|H_{SO}|o\rangle}{E_u - E_o} \qquad (1)$$

The energy lowering thus depends on the interaction of occupied states o with unoccupied states u (via spin-orbit Hamiltonian H_{SO}). HSE06 increases exchange splitting of d-states and pushes unoccupied $d_{xz/yz}$ states far from the Fermi level (Figure 5), which counterbalances the increase of the spin and orbital moments. Thus the differences in calculated values

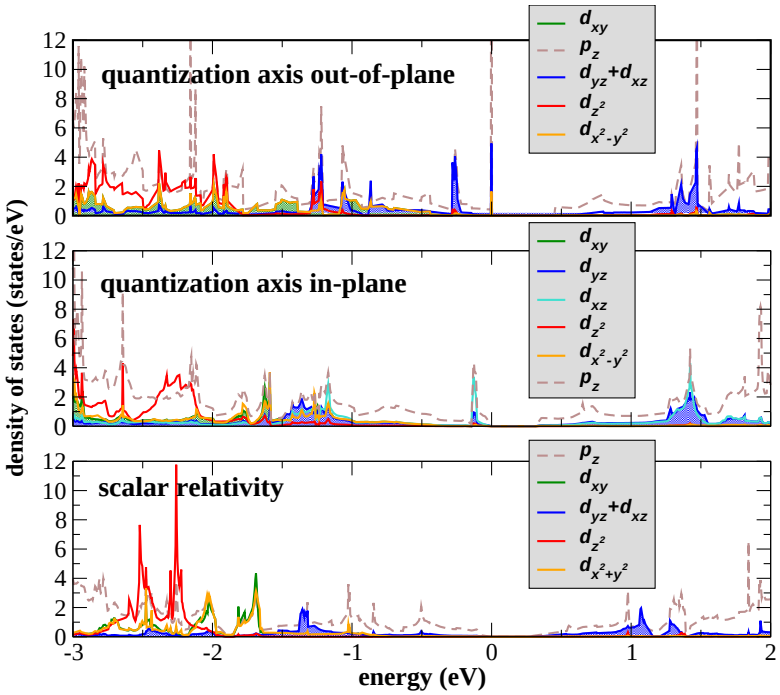

Fig. 6 The density of states of the Ir-graphene complex calculated using HSE06 (hybrid exchange-correlation functional) with a) scalar relativistic approximation b) including spin-orbit coupling with the spin-quantization axis oriented parallel to the graphene sheet (in-plane) c) with the spin-quantization axis aligned perpendicular to graphene (out-of-plane).

stem from different treatment of electron exchange (HSE06 includes non-local Hartree-Fock exchange) and the fact, that the spin-orbit coupling and the intra-atomic exchange are of the same magnitude in 5*d* transition metals.[28]

Although the HSE06 functional reduces the large magnetocrystalline anisotropy energy predicted by functionals utilizing local exchange (LDA and optB86b-vdW), the value of 0.12 kcal/mol is still large to imply the stability of the out-of-plane magnetization. The preference of the out-of-plane easy magnetization is rather exceptional as other 5*d* transition metal atoms adsorbed on graphene prefer in-plane magnetization.[28] The spin and orbital moments in Table 1 reveal that the orbital moments remain the same in both orientations, whereas the spin moments are systematically lower for the in-plane orientation of the spin axis. This result is in contrast to the relation proposed by Bruno[36] that the magnetic anisotropy is proportional to the anisotropy of the orbital moment. However, Bruno's result is derived from the perturbation theory using the assumption that the exchange splitting is much larger that the spin-orbit coupling, which works well for 3*d* transition metals but not for the case of the Ir-graphene system, in which the SOC and exchange splitting are of the same magnitude. The orbital moments are also remarkably insensitive to the choice of the functional, which is in contrast to the large differences observed for the spin moments. It should be noted that, for the in-plane orientation, the convergence of the self-consistent solution of the Kohn-Sham equation was quite problematic and multiple solutions could be found depending on the choice of the initial spin moment, because the energy differences for various magnitudes and directions of the spin moment were very small. Interestingly, the magnetic anisotropy arises from the Ir adatom, because magnetic moments induced on carbon atoms in graphene are negligible ($< 0.01\mu_B$).

Table 1 Spin μ_S and orbital μ_L magnetic moments (in μ_B), magnetocrystalline anisotropy energy (MAE, in kcal/mol) for the Ir-graphene complex; spin-orbit calculation using various functionals with out-of-plane ($\perp$) and in-plane ($\parallel$) orientation of the spin quantization axis

$\mu_S(\perp)$	$\mu_S(\parallel)$	$\mu_L(\perp)$	$\mu_L(\parallel)$	MAE
0.82	0.60	0.31	0.31	0.3
1.49	1.35	0.29	0.30	0.37
1.98	1.65	0.34	0.37	0.12

3 Discussion

Recently, we studied another heavy transition metal-benzene complex, Pt-benzene.[18] The dominant configuration in the Pt-benzene complex is closed-shell singlet, despite the fact that its excitation energy is much higher than the ground state triplet. Triplet state of platinum is quenched also in its complex with graphene.[23] The character and spin multiplicity of the dominant configuration in the complex are particularly important when discussing the doping by heavy transition-metal elements as a way to convert graphene into topological insulator. The spin-orbit interaction is weak in the singlet state, thus Pt adatoms on graphene would hardly make the complex topological insulator.

The Ir-benzene complex shows different behaviour. A pure iridium atom exhibits in the ground-state ^{4}F electronic states arising from $5d^76s^2$ configuration. The first excited state is also quartet ^{4}F, but with $5d^86s^1$ electronic configuration. The excited states of the Ir atom with lower multiplicity are doublet states ^2P and ^2D with $5d^7\ 6s^2$ and $5d^8\ 6s^1$ electron structures, respectively. The CASPT2 calculations predict that, in contrast to the Pt-benzene complex, no change of the spin state occurs after Ir is bound to benzene. The quartet state is stable in the complex along the whole potential energy curve, nevertheless the mixing of quartet states occurs.

The CASPT2 calculation also provides detailed picture of bonding of Ir to benzene. Quartet ^{4}F state with the $5d^86s^1$ electronic configuration is the ground-state in the complex. Notice that the first excited state in the complex is doublet ^2D having the $5d^86s^1$ configuration. The $5d^86s^1$ configuration is energetically advantageous because in the vicinity of the ligand, the occupation of the 6s orbital becomes less favorable due to the Pauli repulsion, whereas the occupation of the 5d orbital is less affected due to the screening of the repulsion in the 5d shell. This electron configuration then binds to the ligand by a dative bond characterized by strong direct charge transfers from iridium d-orbitals to p-states of the ligand and the backward charge transfer to $6p$ orbitals of the Ir atom.

The situation changes when the Ir atom is attached to graphene. The LDA and optB86b-vdW functionals yield the magnetic moment of 0.0 and 0.62 μ in scalar relativistic calculation, respectively, i.e. none of the functionals predicts that the quartet state would remain in the complex. The completely quenched magnetic moment obtained in the LDA calculation arises from charge transfer from the s orbital of the Ir atom into p orbitals of graphene, in addition to the transfer to the d orbitals of Ir creating $5d^86s^1$ electronic configuration. The optB86b-vdW functional reduces the electron transfer to graphene. The optB86b-vdW density of states reveals that there appear half-filled hybridized s-$d_{xz/yz}$ states at the Fermi level, which is the reason for fractional magnetic moment of 0.62 μ. The scalar relativistic calculation with the HSE06 functional yields the net magnetic moment in the complex of 1 μ, which corresponds to the doublet state. Even with spin-orbit coupling, non-collinear magnetic moments in the complex calculated by HSE06 are very close to that of the doublet state. It should be noted here that although hybrid functionals significantly improve the electronic properties of metal-molecule systems, they often lead to a larger exchange splitting and larger magnetic moments for magnetic bulk metals such iron.[37]

According to the density of states the s-states are pushed into unoccupied states and the doublet therefore arises from the $5d^96s^0$ electronic configuration. The HSE06 functional is known to localize the d states in comparison with LDA/GGA functional.[24] The d states - being more localized - sample the potential closer to the nucleus than valence s states, screen the valence s and p states from the nucleus, and, consecutively, push the valence s states further out. It should be noted, that non-zero intrinsic magnetic moment breaks time-reversal symmetry, and therefore topologically non-trivial complex would correspond to a quantum anomalous Hall insulator rather than to a topological insulator. The quantum anomalous Hall insulator, also called Chern insulator, is a state of matter which exhibits a gap in the bulk and chiral gapless edge states at the boundary.[38,39] Notably, it was merely a theoretical concept for a long time, but it has been recently experimentally realized and the gate-tuned anomalous Hall resistance reached the predicted quantized value of h/e^2 at zero magnetic field in agreement with theoretical prediction.[40]

The influence of relativistic effects can be judged by the comparison with the adsorption of cobalt. The cobalt atom has the electron structure very similar to that of iridium; the ground state corresponds to a high-spin quartet state a^4F having the $3d^74s^2$ configuration, the first two excited states are quartet b^4F and doublet a^2F, both with the $3d^84s^1$ configuration. Sargolzaei and Gudarzi[22] studied the adsorption of the Co addatom on benzene and graphene by means of DFT calculation with standard GGA functional.[22] Moreover, Rudenko et al.[41] used the coronene ($C_{24}H_{12}$) to model the face of graphene, which enabled them to employ multi-reference methods: the nonrelativistic CASSCF in conjunction with the strongly contracted variant of the second-order N-electron valence state perturbation theory. Their calculation reveals that as the Co atom approaches the surface, its ground state changes to $3d^84s^1$ quartet at the distance of 2.6 Å and to $3d^94s^0$ (doublet) at shorter distances (1.8 Å). In contrast to the Ir adatom, the global minimum occurs at the potential energy curve of the ground-state $3d^74s^2$ quartet; the two other configurations stay higher in energy over the entire range of distances. The corresponding value of the adsorption energy of 7.4 kcal/mol is quite small compared to the Ir addatom, and this difference can be attributed to relativistic effects; in the free-standing Ir atom, strong relativistic effects contract the 6s

orbitals and, on the other hand, expand 5d orbitals owing to the reduced screening by s orbitals. These two mutual effects result in the *d*-*s* separation of 0.1 eV in the Ir atom, much lower than 0.41 eV in the Co atom.[42] Lower energy penalty for the electron transfer into d orbitals facilitates the creation of the d^8s^1 configuration, which is characteristic for the lowest states in the complex. The different adsorption properties of Co and Ir can be therefore attributed to indirect action of relativistic effects.

The Ir-graphene complex was predicted to be a gapless system without spin-orbit coupling.[9] However, our calculation shows that gapless bandstructure is rather computational artefact of the self-interaction error of the local density functional. The HSE06 functional, in which self-interaction error is reduced by the exact exchange, predicts the gap of 0.3 eV even without spin-orbit coupling. When the spin-orbit interaction is present, the gap size depends on the orientation of the spin quantization axis. Aligning the axis along one of the directions within graphene, the degeneracy of d_{xz} and d_{yz} states is lifted and the gap amounts to 0.31 eV, the value essentially identical to scalar relativistic case. Alignment perpendicular to graphene leads to large gap of 0.45 eV. It should be noted that although hybrid functional greatly improve band gaps over LDA/GGA functionals, one would need to resort to even higher-order approximation to get really accurate values of band gaps. The family of GW methods serves this purpose well, however fully relativistic GW calculation of the Ir-graphene supercell is beyond current computational capacities. The HSE06 result showing that the gap is not opened by the spin-orbit interaction exclusively is illustrative for the issues appearing when DFT is used for treatment of the heavy addatom-graphene complexes. As the systems proposed for the existence of quantum anomalous Hall effect often involve magnetism, localized *d*- or *f*-states, and strong correlations, and one should be aware of the limitations of single-reference local-density DFT methods in these systems.

4 Computational details

Three high symmetry adsorption sites exist on benzene and graphene; on top, directly above a carbon atom, bridge, above the midpoint of a C-C bond, and a so-called hollow site, above the center of the aromatic ring. Our test calculation revealed that Ir prefers the hollow position on benzene, in agreement with previous studies which have shown that the hollow position is preferred by the Ir atom on graphene.[9,28] Thus, we placed the Ir atom into the hollow position in all calculations.

Quantum chemical calculations of the interaction energy, and the nature of bonding of the Ir-benzene complex were performed using multiconfigurational methods. Two different approaches exploiting the multireference Complete Active Space SCF (CASSCF) reference function were utilized; the pertubative CASPT2 approach,[14,15] and its multi-state extension (MS-CASPT2).[43] The interaction energies were corrected for the basis set superposition error (BSSE) using the counterpoise correction.[44] The scalar relativistic contribution has been included by using the second-order spin free Douglas-Kroll-Hess (DKH) Hamiltonian.[45,46]

The methodology of CASSCF/CASPT2 calculations used in this paper follows our previous study focused on the investigation of the Pt-benzene complex.[18] In the CASSCF calculations the 5d and 6s orbitals of iridium with 2p orbitals of carbons perpendicular to the benzene plane were included in the active space. The active space used thus consists of 15 electrons placed in 12 orbitals (15/12); 9 electrons in six orbitals for the Ir atom and 6 electrons in six orbitals for benzene. In the following CASPT2 calculation, the $5p^65d^76s^2$ shells of iridium and all electrons in benzene with an exception of the $1s^2$ electrons of the carbon atoms were correlated. The standard IPEA shift (0.25 au) has been used in all of our CASPT2 calculations.[47] All CASSCF/CASPT2 calculations were carried out using ANO-RCC basis sets[48,49] with VQZP (Ir atom)/VTZP (benzene molecule) contractions. Spin-orbit effects were estimated using the restricted active space state interaction (RASSI) method within the CASSCF/CASPT2/RASSI-SO approach introduced by Roos and Malmqvist.[50–52] In the present study, these calculations were performed with 8 and 14 lowest-lying roots of doublet and quartet spin states, respectively. The MOLCAS 7.2 program package was employed for the calculations.[53] The structure of benzene optimized at the MP2/cc-pVTZ level (C-C and C-H distances were equal to 1.394 Å and 1.082 Å, respectively) was taken from our previous studies[11,18] and kept frozen in all calculations.

The plane-wave (pw) DFT calculations were performed using the projected augmented wave method implemented in the Vienna Ab initio Simulation Package (VASP).[54,55] The energy cutoff for the pw expansion of the eigenfunctions was set to 400 eV. The convergence criterion for the total energies was set to 10^{-6} eV. The Ir-benzene complex was put into large supercell ($14 \times 14 \times 16$ Å) to minimize the interactions of repeated images. The total magnetic moment of the supercell was not constrained. The graphene sheet was modeled using a 4×4 supercell (32 carbon atoms) with a calculated C-C bond length of 1.44 Å. The periodically repeated sheets were separated by 16 Å of vacuum. Single iridium addatom was placed into the graphene supercell, which corresponds to 6.25 % coverage. The Brillouin zone was sampled by the $3 \times 3 \times 1$ k-point grid for the adsorption energy calculations. The densities of states were calculated using a fine grid of $7 \times 7 \times 1$ k-points. Long-range van der Waals (dispersion) interactions, which are absent in standard DFT approaches, were included by means of the van der Waals density functional,[56–58] using recently proposed modified vdW functionals optB86b-

vdW and optB88-vdW.[59] These functionals yielded enthalpies of adsorption of organic molecules on graphene in excellent agreement with experiment.[60] At the same time, they are able to provide typical solid-state properties such as atomization energies and lattice constants with average errors which are similar or better to those of GGA functional.[58]

The effect of the spin-orbit coupling was included into pw DFT calculations by means of relativistic two-component Hamiltonian, as implemented in VASP, which contains spin-orbit coupling and all relativistic corrections up to order α^2 (where α is the fine-structure constant). The spin-quantization axis was aligned either in the direction perpendicular to the benzene/graphene or in the direction parallel to the plane. The total energy difference between magnetic states with the spin moments oriented in the plane and out of plane gives the value of magnetocrystalline anisotropy energy.

5 Conclusions

Calculated potential energy surfaces reveal high affinity of the iridium atom to either benzene or graphene. In the benzene complex, the benchmark MS-CASPT2-SOC method yield the binding energy of 33.1 kcal/mol at the distance of 1.81 Å between the Ir atom and the middle of the benzene ring. The analysis of results reveals that in the global minimum (at the distance of 1.81 Å), there is single dominant configuration, quartet ^{4}F state with $5d^8 6s^1$ electron configuration. DFT functional optimized for van der Waals interactions optB86b-vdW-SOC performs exceptionally well, yielding the binding energy of 34.5 kcal/mol, just slightly higher than CASPT2 result. Results calculated without explicit spin-orbit terms provided similar agreement between optB86b-vdW and MS-CASPT2. Spin-orbit interaction leads only to the lowering of the binding energy. The quartet state of Ir remains the minimum along the potential energy pathway, with or without spin-orbit interaction. The multi-reference character of the Ir-benzene complex expresses itself by appearance of the shallow local minimum of the potential energy at the distance of 3.00 Å. The shallow minimum is not reproduced by any DFT functionals, because it arises from the van der Waals interaction together with the intermixing of close-lying quartet states of Ir. Nevertheless, our results show that the ground-state of Ir atoms adsorbed on arenes can be described by the single-reference methods with a good accuracy.

In the Ir-graphene complex, the binding energy of 24.9 kcal/mol calculated with the optB86b-vdW-SOC method is slightly lower than the binding energy in the Ir-benzene complex. Still, its value surpasses the binding energies of the other noble metal atoms.[11,18,61] The HSE06 calculation of the density of states reveals the gap of 0.3 eV directly at the Fermi level without spin-orbit coupling, whereas both LDA and GGA yield gapless density of states in scalar relativistic limit. The preferred orientation of the spin quantization axis lies along the direction perpendicular to the graphene plane (out-of-plane), in agreement with previous study by Zhang et al.[28] Hybrid functional HSE06 lowers magnetocrystalline anisotropy energy predicted by local functionals (LDA: 0.3, GGA/PBE 0.37 kcal/mol) to a value of 0.1 kcal/mol, which is still several orders of magnitude higher than the magnetocrystalline anisotropy energy of elemental bulk magnets. The magnetization of Ir covered graphene is therefore very stable. The value of the net magnetic moment in the complex of 1 μ calculated by HSE06 corresponds to the doublet state, in contrast to the LDA functional, which predicts that the magnetic moment is almost completely quenched. The intrinsic magnetic moment breaks time-reversal symmetry, and thereby the topologically non-trivial system would correspond to the anomalous Hall insulator rather than to the topological insulator.

6 Acknowledgements

This work was supported by the Operational Program Research and Development for Innovations - European Regional Development Fund (project no. CZ.1.05/2.1.00/03.0058) the Operational Program Education for Competitiveness - European Social Fund (CZ.1.07/2.3.00/20.0017 and CZ.1.07/2.3.00/20.0058) of the Ministry of Education, Youth and Sports of the Czech Republic, and the Grant Agency of the Czech Republic (P208/12/G016).

References

1 K. S. Novoselov, A. K. Geim, S. V. Morozov, D. Jiang, Y. Zhang, S. V. Dubonos, I. V. Grigorieva and A. A. Firsov, *Science*, 2004, **306**, 666–669.
2 A. K. Geim and K. S. Novoselov, *Nat. Mater.*, 2007, **6**, 666–669.
3 K. S. Novoselov, V. I. Falko, L. Colombo, P. R. Gellert, M. G. Schwab and K. Kim, *Nature*, 2012, **490**, 192–200.
4 F. Schwierz, *Nature Nanotech.*, 2010, **5**, 487–496.
5 C. Kane and E. Mele, *Phys. Rev. Lett.*, 2005, **95**, 146802.
6 L. Fu, C. L. Kane and E. J. Mele, *Phys. Rev. Lett.*, 2007, **98**, 106803.
7 M. Z. Hasan and C. L. Kane, *Rev. Mod. Phys.*, 2010, **82**, 3045.
8 V. Georgakilas, M. Otyepka, A. B. Bourlinos, V. Chandra, N. Kim, K. C. Kemp, P. Hobza, R. Zboril and K. S. Kim, *Chem. Rev.*, 2012, **112**, 6156–6214.
9 J. Hu, J. Alicea, R. Wu and M. Franz, *Phys. Rev. Lett.*, 2012, **109**, 266801.
10 A. T. N'Diaye, S. Bleikamp, P. J. Feibelman and T. Michely, *Phys. Rev. Lett.*, 2006, **97**, 215501.
11 J. Granatier, P. Lazar, M. Otyepka and P. Hobza, *J. Chem. Theory Comput.*, 2011, **7**, 3743–3755.
12 J. Granatier, P. Lazar, R. Prucek, K. Safarova, R. Zboril, M. Otyepka and P. Hobza, *J. Phys. Chem. C*, 2012, **116**, 14151–14162.
13 T. Zhang, Q. Xue, S. Zhang and M. Dong, *Nano Today*, 2012, **7**, 180–200.
14 K. Andersson, P.-A. Malmqvist, B. O. Roos, A. J. Sadlej and K. J. Wolinski, *J. Phys. Chem.*, 1990, **94**, 5477.
15 K. Andersson, P.-A. Malmqvist and B. O. Roos, *J. Phys. Chem.*, 1992, **96**, 1218.

16 M. Schreiber, M. R. Silva-Junior, S. P. A. Sauer and W. Thiel, *The Journal of Chemical Physics*, 2008, **128**, 134110.

17 J. E. Sansonetti and W. C. Martin, *J. Phys. Chem. Ref. Data*, 2005, **34**, 15592259.

18 J. Granatier, M. Dubecky, P. Lazar, M. Otyepka and P. Hobza, *J. Chem. Theory Comput.*, 2013, **9**, 1461–1468.

19 W. Liu, J. Carrasco, B. Santra, A. Michaelides, M. Scheffler and A. Tkatchenko, *Phys. Rev. B*, 2012, **86**, 245405.

20 J. P. Perdew, K. Burke and M. Ernzerhof, *Phys. Rev. Lett.*, 1996, **77**, 3865.

21 P. Lazar, S. Zhang, K. Safarova, Q. Li, J. P. Froning, J. Granatier, P. Hobza, R. Zboril, F. Besenbacher, M. Dong and M. Otyepka, *ACS Nano*, 2013, **7**, 1646.

22 M. Sargolzaei and F. Gudarzi, *J. Appl. Phys.*, 2011, **110**, 064303.

23 P. Blonski and J. Hafner, *J. Chem. Phys.*, 2012, **136**, 074701.

24 A. J. Cohen, P. Mori-Sanchez and W. Yang, *Chem Rev.*, 2012, **112**, 289.

25 I. de P. R. Moreira, F. Illas and R. L. Martin, *Phys. Rev. B*, 2002, **65**, 155102.

26 J. Uddin and G. E. Scuseria, *Phys. Rev. B*, 2006, **74**, 245115.

27 C. Franchini, R. Podloucky, J. Paier, M. Marsman and G. Kresse, *Phys. Rev. B*, 2007, **75**, 195128.

28 H. Zhang, C. Lazo, S. Blügel, S. Heinze and Y. Mokrousov, *Phys. Rev. Lett.*, 2012, **108**, 056802.

29 R. J. Xiao, M. D. Kuzmin, K. Koepernik and M. Richter, *Appl. Phys. Lett.*, 2010, **97**, 232501.

30 P. Blonski and J. Hafner, *J. Phys.: Condens. Matter*, 2014, **26**, 146002.

31 E. Y. Tsymbal, *Spintronics: Electric toggling of magnets*, 2011.

32 I. G. Rau, S. Baumann, S. Rusponi, F. Donati, S. Stepanow, L. Gragnaniello, J. Dreiser, C. Piamonteze, F. Nolting, S. Gangopadhyay, O. R. Albertini, R. M. Macfarlane, C. P. Lutz, B. A. Jones, P. Gambardella, A. J. Heinrich and H. Brune, *Science*, 2014, **344**, 988–992.

33 P. Blonski and J. Hafner, *Phys. Rev. B*, 2009, **79**, 224418.

34 I. Beljakov, V. Meded, F. Symalla, K. Fink, S. Shallcross, M. Ruben and W. Wenzel, *Nano Letters*, 2014, **14**, 3364–3368.

35 J. He, P. Zhou, N. Jiao, S. Y. Ma, K. W. Zhang, R. Z. Wang and L. Z. Sun, *Magnetic Exchange Coupling and Anisotropy of 3d Transition Metal Nanowires on Graphyne*, 2014.

36 P. Bruno, *Phys. Rev. B*, 1989, **39**, 865.

37 F. Flores and J. Ortega, in *The Molecule-Metal Interface*, ed. N. Koch, N. Ueno and A. T. S. Wee, John Wiley and Sons, 2013, ch. Basic Theory of the Molecule-Metal Interface.

38 F. D. M. Haldane, *Phys. Rev. Lett.*, 1998, **61**, 2015.

39 R. Yu, W. Zhang, H.-J. Zhang, S.-C. Zhang, X. Dai and Z. Fang, *Science*, 2010, **329**, 61.

40 S.-C. Chang, J. Zhang and X. F. et al., *Science*, 2013, **340**, 167.

41 A. N. Rudenko, F. J. Keil, M. I. Katsnelson and A. I. Lichtenstein, *Phys. Rev. B*, 2012, **86**, 075422.

42 Y. Ralchenko, A. E. Kramida, J. Reader and N. A. S. D. Team, *NIST Atomic Spectra Database (version 3.1.5)*, 2008.

43 J. Finley, P.-A. Malmqvist, B. O. Roos and L. Serrano-Andres, *Chem. Phys. Lett.*, 1998, **288**, 299.

44 S. F. Boys and F. Bernardi, *Mol. Phys.*, 1970, **19**, 553.

45 M. Douglas and N. M. Kroll, *Ann. Phys.*, 1974, **82**, 89.

46 B. A. Hess and P. Chandra, *Phys. Scr.*, 1987, **36**, 412.

47 G. Ghigo, B. O. Roos and P.-A. Malmqvist, *Chem. Phys. Lett.*, 2004, **396**, 142.

48 B. O. Roos, R. Lindh, P.-A. Malmqvist, V. Veryazov and P. O. Widmark, *J. Phys. Chem. A*, 2004, **108**, 2851.

49 B. O. Roos, R. Lindh, P.-A. Malmqvist, V. Veryazov and P. O. Widmark, *J. Phys. Chem. A*, 2005, **109**, 6575.

50 B. O. Roos and P.-A. Malmqvist, *Adv. Quantum Chem.*, 2004, **47**, 37.

51 B. O. Roos and P.-A. Malmqvist, *Phys. Chem. Chem. Phys.*, 2004, **6**, 2919.

52 M. Iliaš, V. Kellö and M. Urban, *Acta Phys. Slov.*, 2010, **60**, 259–391.

53 F. Aquilante, L. De Vico, N. Ferré, G. Ghigo, P.-r. Malmqvist, P. Neogrády, T. B. Pedersen, M. Pitoňák, M. Reiher, B. O. Roos, L. Serrano-Andrés, M. Urban, V. Veryazov and R. Lindh, *J. Comput. Chem.*, 2010, **31**, 224–247.

54 P. E. Blöchl, *Phys. Rev. B*, 1994, **50**, 17953.

55 G. Kresse and D. Joubert, *Phys. Rev. B*, 1999, **59**, 1758.

56 M. Dion, H. Rydberg, E. Schroder, D. C. Langreth and B. I. Lundqvist, *Phys. Rev. Lett.*, 2004, **92**, 246401.

57 G. Román-Pérez and J. M. Soler, *Phys. Rev. Lett.*, 2009, **103**, 096102.

58 J. Klimes, D. R. Bowler and A. Michaelides, *Phys. Rev. B*, 2011, **83**, 195313.

59 J. Klimes, D. R. Bowler and A. Michaelides, *J. Phys.: Cond. Matt.*, 2010, **22**, 022201.

60 P. Lazar, F. Karlicky, P. Jurecka, M. Kocman, E. Otyepkova, K. Safarova and M. Otyepka, *J. Am. Chem. Soc.*, 2013, **135**, 6372–6377.

61 M. Amft, S. Lebegue, O. Eriksson and N. V. Skorodumova, *Journal of Physics: Condensed Matter*, 2011, **23**, 395001.

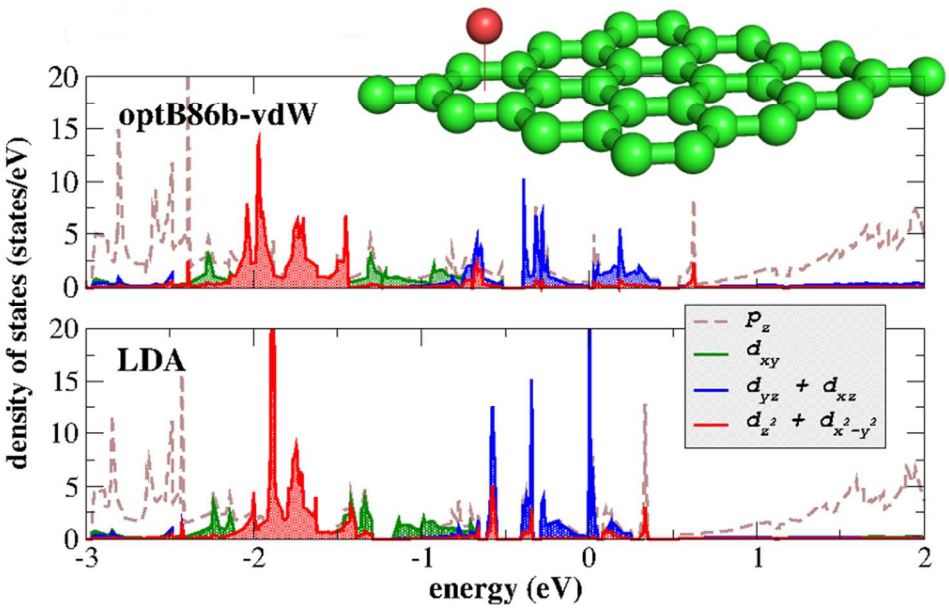

The strong correlation effects contribute to the opening of the band gap in graphene covered with the Ir adatoms.